Journal of Catalysis **187,** 77–84 (1999)
Article ID jcat.1999.2562, available online at http://www.idealibrary.com on IDEAL®

New Nickel Catalysts for the Formation of Filamentous Carbon in the Reaction of Methane Decomposition

M. A. Ermakova,[1] D. Yu. Ermakov, G. G. Kuvshinov, and L. M. Plyasova

Boreskov Institute of Catalysis, Siberian Branch of the Russian Academy of Sciences, Prospekt Ak. Lavrentieva 5, Novosibirsk 630090, Russia

Received January 22, 1999; revised April 7, 1999; accepted May 6, 1999

A method for intentional synthesis of metal catalysts, specifically nickel catalysts for methane decomposition, was developed. The method was based on impregnation of a porous metal oxide with the precursor of a textural promoter followed by reduction of the latter. The desired texture of NiO was provided by precalcining it at a certain temperature within the range 300 to 900°C. A family of nickel-based catalytic systems with various concentrations of the active component, metal particle sizes, and stability to deactivation in the course of synthesis of filamentous carbon was prepared. The yield of carbon and mechanical strength of carbon particles growing on the catalyst during methane decomposition were found to increase with the concentration of nickel in the catalyst, to reach their maxima at 90–96% nickel. The highest yield of carbon (375–384 g carbon per g nickel) was observed for the catalyst with particles of 10–40 nm average diameter. The effect of textural promoters (SiO_2, Al_2O_3, MgO, TiO_2, and ZrO_2) on the catalyst performance was studied; the highest carbon yield was obtained with SiO_2. © 1999 Academic Press

Key Words: **nickel catalysts for methane decomposition; impregnation of porous oxide; textural promoters; yield of filamentous carbon per gram of nickel.**

1. INTRODUCTION

Catalytic filamentous carbon (CFC) is the subject of numerous current studies. A unique filamentous structure of CFC makes it a promising material for various technologies (1–7). First, EM images were recorded for CFC as early as in 1950 (8, 9). In the 1970s, this material was applied as a new promising material. Since that time, the studies in the field have not ceased. Quite extensive literature is available now in the field of CFC. Filaments and nanotubes of various types have been synthesized, and textural and adsorptive properties of this material, as well as kinetics and thermodynamics of CFC formation over some catalysts, have been studied (1, 9–18). A variety of hydrocarbons and catalytic systems for hydrocarbon decomposition have been used for synthesis of CFC of different structures and textures. The pertinent reaction mechanisms have been suggested (19–22). Most of the authors propose CFC as a starting material for synthesis of new adsorbents, composites, and catalysts. Among the other applications, CFC is suggested for use as coats for different materials to vary the properties of the latter (textural parameters, physical properties, catalyst selectivity, etc.). In the meantime, the applicability of CFC to some areas, such as manufacturing of electrodes, lining of rectors and heat exchangers, the metallurgy and chemical industry, pigments and fillers for varnish and paint, electrical and rubber industries, and manufacturing of various lubricants, was not examined. The purity and low price of a product are often of chief importance in these cases. We believe that CFC can be used in these industries. However, there are as yet unresolved problems in the field. Among these problems, which impede the wide application of CFC, is one of manufacturing considerable quantities of this material with reproducible properties.

Notice that little attention is paid in the literature to the problem of the quantitative yield of CFC. Meanwhile, a specific feature of the reaction is that the volume of an initially loaded catalyst is many times increased. And, it must be vigorously stirred during the process, which causes problems even with the scaling of laboratory reactors, not to mention industrial use. Some of approaches to solving this problem are discussed in Ref. (23). Another feature of large-scale CFC production is the use of the cheapest hydrocarbon feedstock such as natural gas with methane as the main component. Therefore, there arises a need for developing highly effective catalysts for decomposition of methane. Iron and nickel are the active components of these catalysts. The nickel-based catalysts are active at lower temperatures and provide a higher yield of CFC per mass unit of the active component. For this reason, the nickel metal-based catalysts seem the most attractive for the industrial use. $Ni–Al_2O_3$ catalysts for methane decomposition prepared by coprecipitating the components were thoroughly investigated (24–26). The highest yield of carbon per catalyst mass unit was obtained using the catalyst comprising 90% nickel, the initial nickel particles of the catalyst being ca. 14 nm in average size. The yield was as high as 145 g carbon per gram of catalyst. Introduction of copper, 3%,

[1] Corresponding author. E-mail: erm@sirius.catalysis.nsk.su.

0021-9517/99 $30.00

to the catalyst allowed the carbon yield to be improved to 240 g per gram of catalyst at some decrease in methane conversion (26).

Deactivation of catalysts for hydrocarbon decomposition is a fundamental problem. The deactivation mechanisms are discussed elsewhere (27, 28). The deactivation is usually accounted for by either crushing of the active particles (atomic erosion or fragmentary dispersing) in the course of the reaction or encapsulation of the metal particle into carbon. The latter reason seems more plausible for methane decomposition. In this case the deactivation rate is affected by diffusion phenomena in the nickel–carbon system and is determined by the rate ratio of formation of carbon atoms to their diffusion toward the deposition sites. Hence, there is some optimal size of active metal species (nickel particles in this case) to provide the longest equilibrium between the rate of formation of atomic carbon species and the rate of carbon diffusion to the aggregation points. However, it is our opinion that distortions in the metal crystal lattice induced by some impurities (for example, intermetallic compounds of the metal and textural promoter) may have additional impact upon the deactivation rate.

The present work was aimed at comprehensive studies of the influence of concentration and dispersion of the active component in the initial catalyst, as well as the nature of a textural promoter, on the time of deactivation of nickel catalysts in the course of methane decomposition to produce CFC.

2. EXPERIMENTAL

Nickel oxide used for preparing nickel catalysts was synthesized by precipitating a nickel nitrate with aqueous ammonia followed by the drying and calcining of the obtained precipitate (nickel hydroxide) in a muffle furnace at 300°C for 4 h. The texture of the produced nickel oxide was varied by calcining it at temperatures 300 to 900°C.

Concentrations of alkali and earth metals in NiO samples were determined using an ionization spectroscopic technique with a BAIRD plasma spectrophotometer. A curve for thermal decomposition of nickel hydroxide was plotted using a Q-1500 derivatograph.

To prepare catalysts, the precursor of an active component (nickel oxide in our case) was impregnated with the solution of the precursor of a textural promoter taken in the calculated amount (29). Hard-to-reduce oxides (HRO) such as silica, alumina, titanium dioxide, zirconium oxide, and magnesia were used as textural promoters. An alcohol solution of tetraethoxisilane (TEOS) was used as the supplier of silica, an aluminium isopropoxide solution in xylene and an aqueous solution of aluminium nitrate as suppliers of alumina, a solution of titanium ethoxide in xylene as the supplier of titanium dioxide, an aqueous solution of zirconyl nitrate as the supplier of zirconium oxide, and an aqueous solution of magnesium nitrate as the supplier of magnesia. The impregnated precursors were dried at room temperature and reduced in hydrogen at 550°C for 1 h. Before being unloaded from the reactor, prepared catalysts were passivated with ethanol in order to prevent pyrophoric phenomena. The TEOS to be introduced into pores of nickel oxide was pre-hydrolyzed with a substoichiometric amount of water with hydrogen chloride added as the hydrolysis catalyst. TEOS molecules were thus coupled together to form oligomer chains through siloxane bonds to allow for the rates of bulk aggregation of SiO_2 particles and of gel formation on storing to be many times decreased. The other solutions were not subjected to any pretreatment procedure.

A sample of 90% Ni–10% Al_2O_3 catalyst used for comparison was prepared by coprecipitation according to the method given elsewhere (26). The components were precipitated by NaOH from an aqueous solution of $Ni(NO_3)_2 \cdot 6H_2O$ and $Al(NO_3)_3 \cdot 9H_2O$ taken in known proportions. Samples were carefully washed with distilled water until no NO_3 ions were detected in the remaining solution and were calcined in flowing nitrogen for 3 h. The calcination temperature was elevated at the rate of ca. 5°C min^{-1} to 350°C. Samples were reduced in flowing pure hydrogen for 3 h at the temperature elevated to 550°C at the same rate.

The texture of samples was characterized by low-temperature nitrogen adsorption at 77 K using an automated installation ASAP-2400.

The average sizes of nickel oxide and nickel metal particles were determined by the Sherrer radiographic method (30) based on the half-width of diffraction lines assigned to (200), (111) NiO and (200), (111) Ni. The XRD technique was used for determining the phase composition of the samples.

The catalysts were tested in a vibrofluidized bed at 550°C using a laboratory installation with a flow quartz reactor. The operation region of the reactor was 20 cm^3 in volume. Methane consumption was always preset at 120 liter per gram of nickel per hour. Hydrogen concentration in the mixture was chromatographically measured using a column filled with NaX zeolite. The catalyst activity was determined from the hydrogen percentage in the reaction mixture. The reaction was stopped as soon as the outlet hydrogen concentration reached 5%. The amount of carbon deposited on the catalyst during the reaction time was determined by weighing unloaded samples.

Attrition resistance of carbon granules was determined by the method described in Ref. (31). A sifted carbon fraction (2–1.25 mm) in the amount 0.2 g was loaded into a conical drum with its wide end of 65 mm diameter rotated at the rate of 2 turns per s. A porcelain ball of 20 mm diameter and 10 g weight was placed into the drum to intensify the attrition process. The test took 6 h; then the sample was unloaded and sifted using a sieve with 1.25 mm mesh.

Attrition was taken equal to the percentage of granules passed through the mesh.

3. RESULTS AND DISCUSSION

3.1. Precursors of Active Component

Concentrations of alkali metals and calcium (<0.03% for K; ca. 0.001% for Na; ca. 0.005% for Ca) not higher than their concentrations in distilled water were determined in nickel hydroxide using ionization spectroscopy. That was why we did not take into account the influence of these metals on catalyst sintering.

X-ray amorphous nickel hydroxide with the specific surface area of 256 m^2/g was produced using the above-described method. During thermal decomposition of it, principal endothermic transformations were observed at 290°C, generally in agreement with the pertinent literature data (24, 32).

Decomposition of nickel hydroxide at 300°C produced nickel oxide with specific surface area 144 m^2/g and average particle size 3–4 nm (from XRD data).

3.2. Influence of Nickel Concentration in the Catalyst on Carbon Yield and Granule Strength

For nickel–alumina catalysts, the yield of carbon per catalyst mass unit was shown (26) to increase with the concentration of nickel in the catalyst. The highest carbon yield, equal to 145 g per gram of catalyst, was reached at 90% Ni. However, the next point was the 100% nickel catalyst comprising no textural promoter. A sharp decrease in capacity to yield carbon, to lower than one tenth, was observed.

In the present work we tried to study the nickel–silica system in the same manner. The system was prepared by a unique method (29). Unlike the method described in Ref. (26), this one provided a wider range, 30 through 96%, of nickel concentrations. Table 1 shows that the yield of carbon per active component mass unit (hereinafter referred to as *carbon yield*) goes through a maximum at the range 90 to 96% nickel, which is in agreement with the conclusions made in Refs. (24–26). The deactivation time of the 90% Ni–10% SiO_2 catalyst, which shows the best performance among the catalysts discussed in the present work, is about three times that observed for the coprecipitated Ni–Al_2O_3 catalyst with the same concentration of nickel (Fig. 1). Accordingly, the carbon yield is also improved. The rate of carbon deposition is ca. 10 g/g Ni h for the nickel catalysts presented in Fig. 1. Then, the carbon yield under these conditions may be calculated as

$$G_C = t_d \times 10,$$

where G_C is the carbon yield and t_d is the lifetime (h) of the catalyst until the complete deactivation.

Notice that in the vibrofluidized catalyst bed, CFC is nucleated and grows in the form of irregularly shaped granules. The granule strength is obviously dependent on the nickel loading in the catalyst. The granule strength is seen in Fig. 2 to increase with an increase in the nickel concentration. Probable reasons are as follows. The lower the nickel

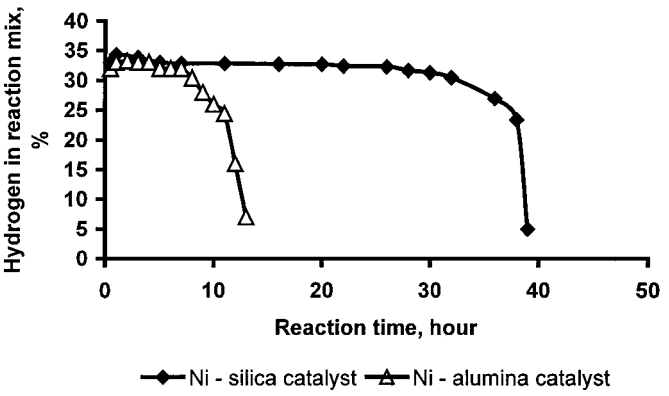

FIG. 1. Activity (% H_2) of coprecipitated nickel–alumina catalyst and nickel–silica catalyst, prepared from NiO calcined at 450°C, vs reaction time.

TABLE 1

Influence of Nickel Concentration (%) in Ni–SiO_2 Catalysts, Prepared by Calcining NiO at 300°C, on the Surface Area (S_{specif} cat, m^2/g) of Reduced Catalysts, the Size of Metal Particles (D_{Ni}, nm), the Carbon Yield (G_c, g CFC/g Ni), and the Specific Surface Area of CFC ($S_{specif\ CFC}$, m^2/g)

% Ni	S_{specif} cat	D_{Ni}	G_c	$S_{specif\ CFC}$
30	583	7	120	124
50	360	9	220	133
70	210	9	183	146
85	120	10	204	130
90	71	11	300	100
96	49	23	238	106
100	6	65	10	—

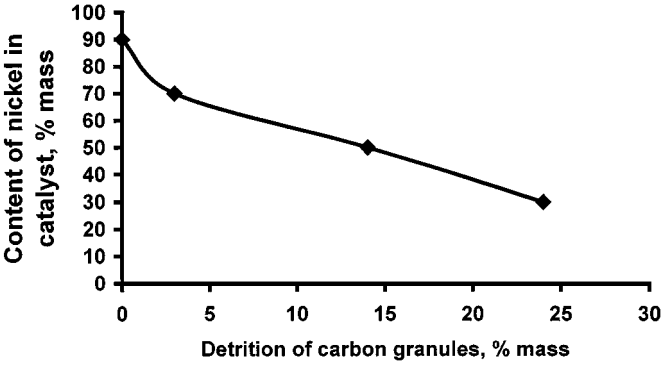

FIG. 2. Effect of nickel concentration in the catalyst on attrition resistance of carbon granules deposited on this catalyst.

concentration is in the initial catalyst, the longer is the distance between the carbon filaments growing on the active species and the lower is their concentration per unit volume of the carbon granule. Thus, the density and, hence, the strength characteristic of the carbon formed on high-loaded nickel catalysts cannot be reached on the low-loaded catalyst at the moment of the catalyst deactivation. Again, the strength and density of carbon granules also depend on the carbon yield provided by the catalyst. The higher the carbon yield, the higher the density of it. For example, the pore volume equals 0.27 cm^3/g in the carbon produced on 90% Ni–10% SiO_2 (at the carbon yield of 300, see Table 1), but it equals 0.34 cm^3/g in the carbon synthesized on 30% Ni–70% SiO_2 (at the carbon yield of 120). There is an apparent difference between the strengths of these carbon samples (Fig. 2).

One can also assume, based on the data available in Table 1 for the given series of catalysts, that the carbon yield is affected by the nickel particle size and reaches a maximum at the average diameter equal to 10–20 nm. It also should be notice that somewhat of a decrease in the specific surface area of CFC is observed at the maximal nickel concentration in the catalyst and the maximal carbon yield. This effect is, probably, the result of an increase in the diameter of carbon filaments.

3.3. Influence of Average Size of Nickel Particles on Carbon Yield

The influence of the size of active particles on the carbon yield was studied thoroughly using a series of catalytic systems with the same proportions of components but different average diameters of nickel particles. The catalysts were synthesized by a unique method. A nickel oxide sample was divided into eight portions, and each of them was calcined at temperatures ranging from 300 to 900°C in order to prepare precursors of the active component with a preset texture. Figure 3 shows specific surface area of NiO against the calcination temperature.

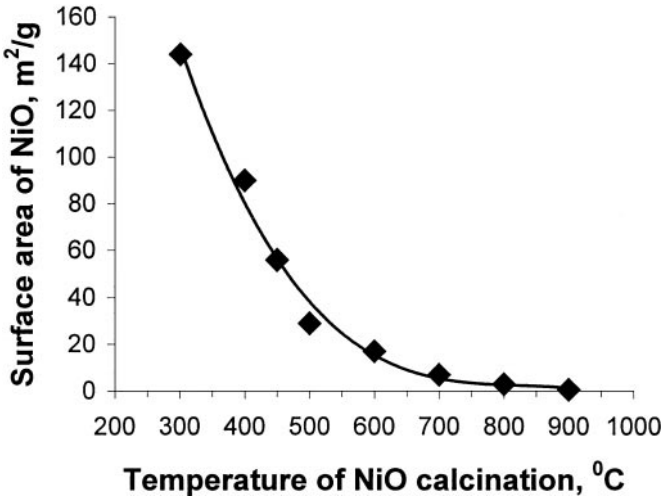

FIG. 3. NiO specific surface area as a function of calcination temperature.

Thus, oxide systems comprising NiO particles of average diameter from 3 to more than 100 nm were synthesized (Table 2). Stabilization of the obtained textural parameters was achieved by impregnating the oxide systems with SiO_2 in amounts of 4 to 10%. As was to be expected, reduction of the catalysts by hydrogen demonstrated that NiO particles to be reduced to the metal state are stabilized more reliably at a higher proportion of SiO_2. For example, when the oxide particles are 4 nm in average size, the proportion of silica of 4% was, apparently, insufficient to prevent them from sintering, and the diameter of the formed metal particles was almost 7–8 times that of the precursor particles. At the same time, the sintering process resulted in no more than a fourfold increase in the diameter of the primary particles in the presence of 10% silica. As the size of the primary NiO particles increased, the stabilizing effect was equalized and became independent of the proportion of introduced silica. As for the carbon yield, the highest capacity to yield carbon was observed for the systems comprising 10%

TABLE 2

Influence of Temperature of Nickel Oxide Calcination on Textural Parameters of Ni Catalysts and the Carbon Yield (G_C, g CFC/g Ni), Particle Size (D_{NiO}, nm), Specific Surface Area (S_{specif}, m^2/g), Pore Volume (V_{pore}, cm^3/g), Average Pore Size (D_{pore}, nm)), and size of metal particles (D_{Ni}, nm)

$T_{calcin.}$ NiO (°C)	$S_{specif.}$ NiO	V_{pore}	D_{pore}	D_{NiO}	96% Ni–4% SiO_2		90% Ni–10% SiO_2	
					D_{Ni}	G_C	D_{Ni}	G_C
300	144	0.57	17	3	23	238	10	300
400	90	0.40	18	12	20	238	10	375
450	56	0.28	20	19	20	300	17	375
500	29	0.15	20	35	25	224	25	340
600	17	0.05	20	40	32	200	30	370
700	7	0.03	20	65	38	107	40	384
800	3	0.013	20	88	—	1.5	—	2
900	0.7	—	—	>100	—	0.5	—	0.5

silica and particles of 10 to 40 nm average size. The further increase in the average size of nickel particles resulted in a sharp decrease in the amount of carbon deposited thereon. Thus, silica introduced according to the above-described procedure can be considered as an effective textural promoter to provide synthesis of the catalytic system with the required textural parameters. Therefore, the given method can be used for preparing catalysts with preset parameters and for other reactions.

3.4. *Effect of Chemical Nature of the Textural Promoter in Nickel Catalysts on the Carbon Yield*

The effect of the chemical nature of textural promoters introduced into a catalytic system on the efficiency of nickel catalysts was studied with respect to the reaction of methane decomposition to produce filamentous carbon. Two series of nickel catalysts were prepared by calcining NiO at 300 and 450°C, respectively. The oxide calcined at the minimal temperature (300°C) was shown above to consist of the finest particles of NiO (ca. 3 nm). Hence, impregnation of this oxide with various HRO can illustrate the efficiency of these compounds as textural promoters protecting the metal particles against sintering in the course of the reduction. This knowledge may be useful to develop high-loaded metal catalysts comprising active particles of the minimal size. However, methane decomposition needs catalytic systems with coarser particles. These particles are formed when NiO calcined at temperatures above 400°C is used as the catalyst precursor. SiO_2, ZrO_2, MgO, TiO_2, and Al_2O_3 were introduced into oxide matrices. Note that alumina was introduced into the NiO pores from the solutions of various compounds. The interaction between alumina, prepared by decomposition of aluminium isopropoxide, and nickel oxide was unlikely to produce chemical compounds, whereas such a potentiality was not excluded to occur during impregnation of nickel oxide with an aqueous solution of aluminium nitrate. These phenomena may affect the texture of the catalysts upon further treatments. Later, the essential difference between the catalyst prepared using aluminium isopropoxide and that prepared from aluminium nitrate was found.

Table 3 presents the data on the size of metal particles and the carbon yield obtained over the corresponding catalysts. What is seen for the catalyst prepared using nickel oxide precursor calcined at 300°C is as follows:

(a) The highest level of protecting metal particles against sintering during the reduction is achieved in the presence of SiO_2. In this case, the particles formed are as little as 3 or 4 times coarser relative to the average size of the precursor (NiO) particles;

(b) Al_2O_3 and TiO_2 used as the textural promoter provided the lowest level of protecting Ni particles against sintering;

TABLE 3

Effect of the Nature of Textural Promoter on the Size of Metal Particles (D_{Ni}, nm) in the Reduced 90% Nickel Catalysts and the Carbon Yield (G_c, g CFC/g Ni)

	T of NiO calcination 300°C		*T* of NiO calcination 450°C	
Promoter	D_{Ni}	G_c	D_{Ni}	G_c
SiO_2	11	300	17	375
Al_2O_3	28	220	22	315
Al_2O_3[a]	43	20	20	280
ZrO_2	16	272	21	300
TiO_2	30	200	26	218
MgO	17	220	22	287

[a] Al_2O_3 was introduced into the nickel oxide matrix from the aqueous solution of aluminum nitrate.

(c) Intermediate efficiency was observed with MgO and ZrO_2 as textural promoters.

When NiO calcined at 450°C was the catalyst precursor, the sintering processes were confined to the inside of the paternal particles of ca. 19 nm, whatever textural promoter among those under consideration was used. Figure 4 demonstrates diffraction patterns recorded for 90% Ni catalysts with various textural promoters and for oxide nickel precursor of these catalysts. Broadening of the (111) and (200) lines used by us to compute the average size of nickel particles is seen to be approximately equal for all the catalytic systems and to correspond to broadening of the (111) line of nickel oxide. Nevertheless, the highest carbon yield was observed with the Ni–SiO_2 catalysts. It seems appropriate to explain this phenomenon in terms of the presence or absence of intermetallic Ni–HRO compounds in the system, which may effect the process of carbon diffusion through the nickel particle. Notice that no unambiguous solution of this problem is available in the literature. The authors' opinions are quite contradictory. For example, the presence of chemical compounds which inhibit decomposition of hydrocarbons is assumed in the Ni/SiO_2 systems (33–35). On the other hand, the authors of Refs. (36, 37) believe that intermetallic Ni–Si compounds cannot be formed at temperatures below 1000 K, and Ni is only preserved in the metal state. It is our opinion (which agrees with the understanding of other authors (32)) that the interaction between the components is minimal in the Ni–SiO_2 system compared to that in the other systems, e.g., Ni–Al_2O_3, with any method used for preparing the catalysts. This kind of interaction is even less probable in the catalysts prepared by the method proposed by us because the textural promoter precursor is introduced into the calcined preformed NiO. At this stage any interaction of the components may hardly occur when tetraethoxisilane is used as the precursor of HRO. Again, the following stage of reduction in hydrogen

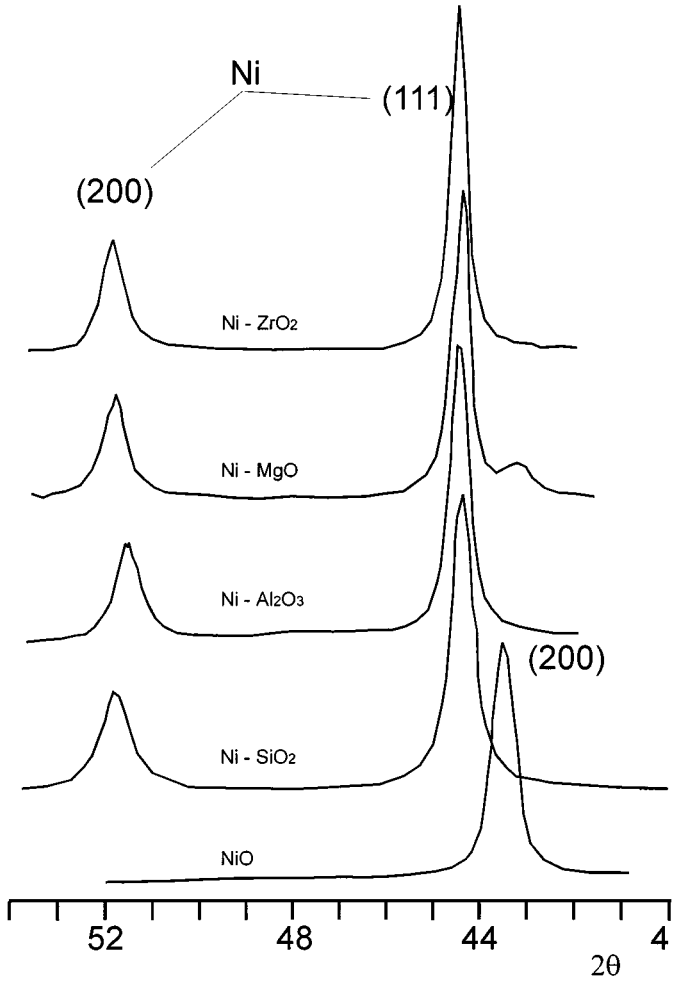

FIG. 4. Diffraction patterns of NiO calcined at 450°C and catalysts prepared thereof.

at a high rate of temperature elevation (no less than 20°C/min) does not allow these compounds to be formed. Some of our catalyst samples comprising 85% Ni and 15% SiO_2 were studied using mass-spectrometry of secondary ions. This is a very sensitive technique, but we failed to detect any Ni–Si compound in the catalyst reduced in hydrogen at 550°C. On the contrary, the paracrystallinity of nickel was revealed in the Ni–Al_2O_3 catalyst for methane decomposition (25) due to the penetration of the hard-to-reduce oxide into the crystal nickel lattice, the effect of the paracrystal nickel state being not related to the carbon yield in this reaction. However, from the data by the same authors (26), the average size of nickel particles falls into the optimal range determined by us but the carbon yield is not higher than 145 g per gram of catalyst. The coprecipitation method used to prepare these catalysts is known to favor a strong interaction between the components and, in this case, the formation of spinels which are not reduced even at a temperature as high as 550°C. Addition of a minor amount of copper, which is known to promote reduction of transition metals, resulted in remarkable improvement of the carbon yield (26). Thus, the above discussion allows the conclusion that the yield of carbon produced by methane decomposition depends on the purity of nickel particles; the lower is the concentration of distortions of the crystal lattice induced by unreduced intermetallic compounds, the higher is the yield.

If we return to the catalytic systems presented in Table 3, the best performance of the Ni–SiO_2 system may be also accounted for by the lowest density of silica among the HRO under study. The density is 2.65 cm^3/g for quartz, while it is 3.96 cm^3/g for Al_2O_3, 3.58 cm^3/g for MgO, 4.3 cm^3/g for TiO_2, and as high as 5.68 cm^3/g for ZrO_2. Therefore, at the same weight ratio of the constituents (90% Ni and 10% HRO), the Ni–SiO_2 catalyst comprises 27 vol% silica, which is much higher than the volume proportion of HRO in the other systems under consideration: 20 vol% for Al_2O_3, 22 vol% for MgO, 19 vol% for TiO_2, and 15 vol% for ZrO_2. This fact is of great importance because the catalytic system may become rather mobile in the methane medium (38, 39). This is the case in which the higher volume of the textural promoter is to prevent more effectively the sintering of the nickel particles at the earliest stage of the reaction.

3.5. Principle of Catalyst Formation

In coprecipitated high-loaded metal catalysts, the active phase in the catalyst grain may be in the form of individual clusters divided by a textural promoter or in the form of an *infinite cluster* with the embedded textural promoter species (24). Actually, these are extreme cases which coexist. In other words, there occur both individual metal particles and interconnected groups of such particles in the catalytic system at practically any phase ratio. As a result, there must be a wide diameter distribution of active particles. For decomposition of hydrocarbons, the stable reaction can be provided by particles that are neither too fine nor too coarse. The finest particles on which formation of CFC was observed were 2 to 4 nm in size (14, 40). However, it is hardly possible to say anything about any quantitative yield of carbon. As for coarser particles, they become enclosed into the solid carbon crust a in short time during the reaction and, therefore, are deactivated (41, 42). One can assume that a more uniform system is produced by the method we proposed that results in a more narrow range of diameter distribution of the metal particles. This conclusion is based on the following speculations: Hydrolysis of nickel ammoniate results in formation and existence for a while of nickel hydroxide sol with particles of close size, 3–4 nm. The particles are not enlarged in the course of the topochemical reaction $Ni(OH)_2 \rightarrow NiO$. The specific surface area decreases due to an increase in the density of NiO formed (8.91 cm^3/g) against the density of $Ni(OH)_2$ (4.1 cm^3/g). No textural promoter being in the system that time, there is nothing to hinder the nickel oxide particles from

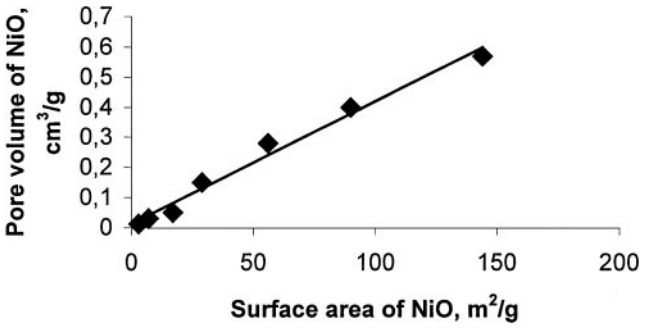

FIG. 5. Pore volume of NiO samples, calcined at various temperatures, vs specific surface area.

further enlargement, which depends on thermodynamic factors only, such as temperature and calcination time. Thus, highly dispersed NiO particles (which are formed at the minimal temperature, 300°C, of decomposition of nickel hydroxide) coalesce in uniform manner at the sites of contacts at elevating temperature and the system remains uniform. The NiO pore volume is proportional to a decrease in the specific surface area (Fig. 5), the average pore diameter being practically unchanged (Table 2). At first glance, such a phenomenon seems improbable, while numerous literature data, e.g., those cited in Refs. (43–47), argue the same to be observed upon thermal shrinkage of silica. Iler (47) attributes this phenomenon to the formation, as a result of sintering, of local regions evenly distributed through the bulk of silica, which are free of pores, or the pores are not exposed to adsorbate molecules. The further elevation of the calcination temperature results in formation of new regions, and the like. Such a NiO system seems to resemble silica, which is known to be a uniform system. The system can be stabilized at a certain stage by impregnating it with an HRO precursor. As a result, HRO molecules are adsorbed on energetically favorable fragments of the oxide surface (Fig. 6), viz. bridges between the particles to prevent them from further coalescing. The stabilizing role of these compounds is very significant, so the average size of nickel oxide particles does not change upon calcining the system at a temperature as high as 800°C, whereas the particles are about 5 times increased in the absence of HRO at the same calcination temperature. The stabilizing feature of HRO during the reduction is more pronounced, the smaller is its particle size relative to the size of particles to be stabilized. That is why the complete stabilization of the finest NiO particles cannot be achieved due to the close sizes of HRO and NiO particles. Nevertheless, sintering can be avoided in the most cases (see Tables 2 and 3).

Thus, one can assume that the prepared catalytic system is built-up by rather uniform metal particles joining one another to form an infinite cluster. HRO particles are allocated among the pores between them and behave as the textural promoter. Such a structure is independent of the metal-to-HRO percentage ratio. This is the fundamental difference between the systems under consideration and those obtained by coprecipitation. Theoretically, the only parameters affecting the amount of the introduced textural promoter are the concentration of the HRO precursor in the impregnating solution and the pore volume of the active component precursor. In practice, the uniform mode of HRO distribution in the subsurface region of the active phase will be inevitably disrupted as the HRO concentration increases above a certain level.

Essentially, the catalytic systems discussed above resemble impregnated catalysts but bear an opposite sense. Both cases imply impregnation of a preformed solid matrix with a liquid phase and adsorption of the solute on the surface followed by thermal decomposition of this compound. As for our case, the solid matrix being considerably transformed during the reduction, the process of formation of the catalytic system is more complicated and needs further study. Nevertheless, the stabilizing effect of the textural promoter introduced in such a manner is rather high, which allows the coalescing of the metal particles to be avoided in many cases under severe reduction conditions, even though the particles are in direct contact with one another.

4. CONCLUSIONS

The following conclusions can be made based on the results obtained:

(1) A unique method was developed for intentional synthesis of metal catalysts, specifically nickel catalysts for methane decomposition. The method allows the catalytic systems to be synthesized in a wide phase range (active

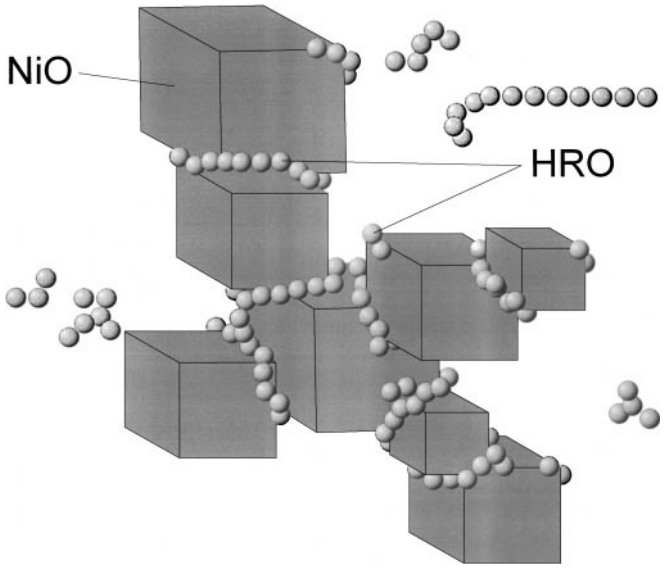

FIG. 6. Hard-to-reduce oxide arrangement in the structure of NiO matrix.

component to HRO ratio) and, on the other hand, active particles of the required size to be obtained at the same phase ratio.

(2) The carbon yield and the strength of granules deposited on the catalyst upon methane decomposition were shown to increase with an increase in the nickel concentration in the catalyst to reach a maximum in the range 90 to 96% Ni.

(3) The maximal carbon yield was shown to be attained with the catalysts comprising a textural promoter in the amount of 10% and active particles of 10 to 40 nm average diameter.

(4) Comparative studies of the stabilizing effect of various textural promoters (SiO_2, Al_2O_3, MgO, TiO_2, and ZrO_2) demonstrated that the highest carbon yield (375 g) was obtained with SiO_2. Not far worse results were obtained with the other textural promoters if the NiO precursor was treated at the optimal temperature. It should be emphasized that the method used for preparing these catalytic systems provides a minor chemical interaction between the constituents. We think that this feature favors the maximal carbon yield.

ACKNOWLEDGMENTS

The authors are grateful to Professor V. B. Fenelonov for the adsorption studies.

REFERENCES

1. Baker, R. T. K., *Carbon* **27**(3), 315–327 (1989).
2. Rodriguez, N. M., *J. Mater. Res.* **8**(12), 3233–3250 (1993).
3. Kuvshinov, G. G., Avdeeva, L. B., Goncharova, O. V., and Mogilnykh, Yu. I., *in* "Extended Abstracts, ACHEMA'94 International Meeting on Chemical Engineering and Biotechnology, Thermal Process Engineering, Frankfurt on Main, 5–11 June 1994," paper 9.6., 1994.
4. Shaikhutdinov, Sh. K., Zaikovskii, V. I., and Avdeeva, L. B., *Appl. Catal. A* **148**, 123–133 (1996).
5. Fenelonov, V. B., Avdeeva, L. B., Zheivot, V. J., Okkel, L. G., Goncharova, O. V., and Pimneva, L. G., *Kinet. Katal.* **34**, 545 (1993).
6. Kim, M. S., Rodriguez, N. M., and Baker, R. T. K., *in* "Synthesis and Properties of Advanced Catalytic Materials" (E. Iglesia, P. W. Lednor, D. A. Nagaki, and L. T. Thompson, Eds.), MRS Symp. Proceedings, Vol. 368, p. 99, 1994.
7. Molchanov, V. V., Chesnokov, V. V., Buyanov, R. A., and Zaizeva, N. A., *Kinet. Katal.* **39**(3), 407–415 (1998).
8. Watson, J. H. L., Leger, A. E., and Oulett, J., *Phys. Colloid Chem.* **54**, 969 (1950).
9. Watson, J. H. L., Vanpu, M., and Lind, S. S., *Phys. Colloid Chem.* **54**, 391 (1950).
10. Kim, M. S., Rodriguez, N. M., and Baker, R. T. K., *J. Catal.* **134**, 253–268 (1992).
11. Snoeck, J. W., Froment, G. F., and Fowles, M., *J. Catal.* **169**, 240–249 (1997).
12. Shoeck, J. W., Froment, G. F., and Fowlest, M., *J. Catal.* **169**, 250–262 (1997).
13. Alstrup, J., *J. Catal.* **109**, 241–251 (1988).
14. Zaikovskii, V. I., Chesnokov, V. V., and Buyanov, R. A., *Appl. Catal.* **38**, 41–52 (1988).
15. Kuvshinov, G. G., Mogilnykh, Yu. I., and Kuvshinov, D. G., *Catal. Today* **42**, 357–360 (1998).
16. Kuvshinov, G. G., Mogilnykh, Yu. I., Kuvshinov, D. G., Zaikovskii, V. I., and Avdeeva, L. B., *Carbon* **36**, 87–97 (1998).
17. Mogilnikh, Yu. I., Kuvshinov, G. G., and Lebedev, M. Yu., "Conference Eurocarbon '98, Extended Abstracts and Programme, Strasburg, France, July 5–9, 1998," Vol. 1, pp. 445–446, 1998.
18. Rodriguez, N. M., Chambers, A., and Baker, R. T. K., *Langmuir* **11**, 3862–3866 (1995).
19. Chambers, A., Nemes, T., Rodriguez, N. M., and Baker, R. T. K., *J. Phys. Chem.* **102**, 2251–2258 (1998).
20. Sacco, A., Thacker, P., Jr., Chang, T. N., and Chiang, A. T. S., *J. Catal.* **85**, 224–236 (1984).
21. Baker, R. T. K., Barber, M. A., Harris, P. S., Feates, F. S., and Waite, R. J., *J. Catal.* **26**, 51–62 (1972).
22. Buyanov, R. A., Afanasjev, A. D., and Chesnokov, V. V., *Kinet. Katal.* **18**, 839 (1977).
23. Kuvshinov, G. G., Zavarukhin, S. G., Mogilnikh, Yu. I., and Kuvshinov, D. G., *Khim. Prom.* **5**, 300–305 (1998).
24. Goncharova, O. V., Avdeeva, L. B., Fenelonov, V. B., Plyasova, L. M., Malakhov, V. V., Litvac, G. S., and Vlasov, A. A., *Kinet. Katal.* **36**(2), 293–298 (1995).
25. Shaikhutdinov, Sh. K., Avdeeva, L. B., Goncharova, O. V., Kochubey, D. I., Novgorodov, B. N., and Plyasova, L. M., *Appl. Catal. A* **126**, 125–139 (1995).
26. Avdeeva, L. B., Goncharova, O. V., Kochubey, D. I., Novgorodov, B. N., Plyasova, L. M., and Shaikhutdinov, Sh. K., *Appl. Catal. A* **141**, 117–129 (1996).
27. Kuijpers, E. G. M., Tjepkema, R. B., and Geus, J. W., *J. Mol. Catal.* **25**, 241–251 (1984).
28. Tibbetts, G. G., Devour, M. G., and Rodda, E. J., *Carbon* **25**(3), 367–375 (1987).
29. Ermakova, M. A., Ermakov, D. Yu., Kuvshinov, G. G., and Plyasova, L. M., *Kinet. Katal.* **5**, 796 (1998).
30. Guinier, A., "Theorie et Technique de la Radiocristallographie." Dunod, Paris, 1956.
31. Kuvshinov, G. G., Mogilnykh, Yu. I., Kuvshinov, D. G., Ermakov, D. Yu., Ermakova, M. A., Salanov, A. N., and Rudina, N. A., *in* "Symposium on Microscopic Studies of Coal and Carbon, August 22–27, 1998," American Chemical Society Division of Fuel Chemistry Preprints of Symposia, Vol. 43, No. 4, pp. 946–950. Am. Chem. Soc., Washington, DC, 1998.
32. Noskova, C. P., Ph.D. thesis, Novosibirsk, Boreskov Institute of Catalysis, 1975.
33. Zhao, Y. X., Bovers, C. W., and Spain, J. L., *Carbon* **26**, 291 (1988).
34. Kepinnski, L., *Carbon* **30**, 949 (1992).
35. Nakayama, T., Arai, V., and Nishiyama, Y., *J. Catal.* **87**, 108 (1984).
36. Weissman, J. G., Ko, E. J., and Wynblatt, P., *J. Catal.* **125**, 9 (1990).
37. Lamber, R., Jeager, N., and Schulz-Ekloff, G., *Surf. Sci.* **227**, 268 (1990).
38. Rostrup-Nielsen, J. R., *J. Catal.* **85**, 31–43 (1984).
39. Krivoruchko, O. P., and Zaikovskii, V. I., *Kinet. Katal.* **39**(4), 607–617 (1998).
40. Speck, J. S., Endo, M., and Dvesselhaus, M. S., *J. Cryst. Growth* **94**(4), 834 (1989).
41. Audier, M., Bowen, P., and Jones, W., *J. Cryst. Growth* **63**, 125 (1983).
42. Guinot, J., Audier, M., Coulon, M., and Bonnetain, L., *Carbon* **19**, 95 (1981).
43. Teichner, S. J., Nicolaon, G. A., Vicarini, M. A., and Gardes, G. E. E., *Adv. Colloid Interface Sci.* **5**, 245 (1976).
44. Van Nordstrand, R. A., Kreger, V. E., and Ries, H. E., Jr., *J. Phys. Colloid Chem.* **55**, 641 (1951).
45. Bastick, J., *Bull. Soc. Chim. Fr.* **20**, 437 (1953).
46. Kohlschutter, H. W., and Kampf, G., *Z. Anorg. Chem.* **292**, 298 (1957).
47. Iler, R. K., "The Chemistry of Silica." Wiley, New York, 1979.